

Excitation spectrum and momentum distribution of the extended Bose-Hubbard model

Hiroki Nishizawa

Department of Applied Physics, The University of Tokyo, Hongo, Tokyo 113-8656, Japan

(Dated: August 3, 2022)

We investigate the extended Bose-Hubbard model with the nearest-neighbor repulsion on a square lattice by the standard basis operator method. We derive Green's functions in random phase approximation and calculate the excitation spectrum and momentum distribution in Mott insulator, charge density wave, superfluid, and supersolid phases. The excitation spectrum has gapped modes and gapless Goldstone modes in the superfluid and supersolid phases. The momentum distribution has a peak at the zone corner in the supersolid phase and the charge density wave phase close to the phase boundary.

I. INTRODUCTION

The Bose-Hubbard model (BHM) [1, 2] describes bosonic atoms in optical lattices. Since parameters of optical lattices can be tuned flexibly, the BHM is ideal for the investigation of many-body effects. This model undergoes the phase transition from a superfluid (SF) phase to a Mott insulator (MI) phase at the critical ratio of the onsite repulsion to the hopping amplitude [3–5]. These phases are characterized by the excitation spectrum. In the MI phase, all excitation modes are gapped. In contrast, in the SF phase, the spectrum consists of gapped and gapless Goldstone modes [6–14]. The momentum distribution is also an indicator of the SF-MI phase transition. In the SF phase, the momentum distribution has a sharp peak at zero momentum, which indicates the existence of Bose-Einstein condensation and superfluidity [6, 14–17].

The extended Bose Hubbard model (EBHM) is the BHM with nearest-neighbor interactions [18]. The nearest-neighbor repulsion gives rise to solid-ordered phases: a charge density wave (CDW) phase and a supersolid (SS) phase [19, 20]. Although there are many studies on the phase diagram of the EBHM [18–26], there are limited studies on the excitation spectrum and momentum distribution of the EBHM in two and three dimensions. In one dimension, the excitation spectrum has been calculated by the density-matrix renormalization-group method [27]. In two dimensions, the excitation spectrum of the EBHM on a square lattice has been studied by the dynamical Gutzwiller approach [21], but only low-energy excitations have been calculated. The excitation spectrum was also studied based on equations for Green's functions [28], but the solutions of the equations were not presented. Thus, explicit representations of Green's functions were not given, and a method to calculate the excitation spectrum was not explained. The momentum distribution of the EBHM on a square lattice has been calculated in the MI and CDW phases by the strong-coupling perturbation theory [29] and in the SS phase by quantum Monte Carlo simulations [30]. However, differences between the MI, CDW, SF, and SS phases have not been explored.

In this paper, we investigate the EBHM on a square lattice by the standard basis operator (SBO) method. The SBO method has been applied to the BHM in both the MI and SF phases [12–14, 31]. We extend the SBO method to the EBHM on a bipartite square lattice, which has two sublattices due to a periodic density modulation. In Sec. II, we summarize the mean-field phase diagram of the EBHM. In Sec. III, we derive equations for Green's functions by the SBO method in random phase approximation. By solving the equations, we obtain the Green's functions in the MI, CDW, SF, and SS phases. In Sec. IV, we calculate the excitation spectrum that has gapped and gapless modes in the SF and SS phases. In Sec. V, we calculate the momentum distribution that has a peak at the zone corner in the SS phase and the CDW phase close to the CDW-SS phase transition.

II. MEAN-FIELD PHASE DIAGRAM

In this section, we summarize the phase diagram of the extended Bose-Hubbard model [22, 23, 30].

$$H = -t \sum_{\langle ij \rangle} (b_i^\dagger b_j + \text{H.c.}) + \frac{U}{2} \sum_i n_i (n_i - 1) + V \sum_{\langle ij \rangle} n_i n_j - \mu \sum_i n_i, \quad (1)$$

where b_i^\dagger and b_i are the boson creation and annihilation operators at site i , $n_i = b_i^\dagger b_i$ is the number operator, t is the hopping amplitude, U is the onsite repulsion, V is the nearest-neighbor repulsion, μ is the chemical potential, and $\langle ij \rangle$ denotes the summation over the nearest-neighbor sites. The ground state in the atomic limit ($t = 0$) is determined exactly depending on the ratio zV/U , where z is the lattice coordination number ($z = 4$ for a square lattice). When $zV/U > 1$, the ground state is a CDW state. In this phase, $\langle n_i \rangle \neq \langle n_j \rangle$ when i and j are nearest-neighbor sites. The ground state is labeled by (n_A, n_B) , which represents the expectation values of number operators on sublattices A and B . Without loss of generality, we can assume $n_A \geq n_B$. The ground state is $(n, 0)$ for $(n - 1)U \leq \mu \leq nU$.

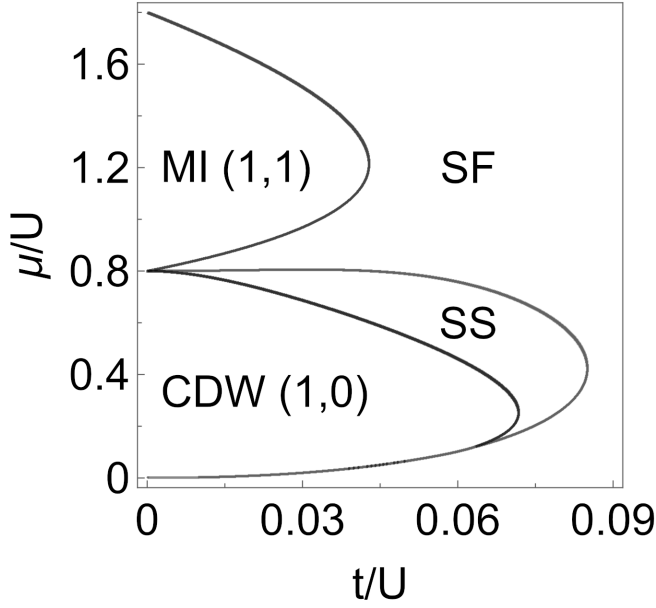


FIG. 1. Phase diagram of the extended Bose-Hubbard model on a square lattice ($z = 4$) for $V/U = 0.2$ at zero temperature by the mean-field approximation.

In contrast, when $zV/U \leq 1$, the ground state alternates between CDW and MI phases as μ increases. The ground state is the CDW state with $(n+1, n)$ for $nU + nzV \leq \mu \leq nU + (n+1)zV$ and the MI state with (n, n) for $(n-1)U + nzV \leq \mu \leq nU + nzV$. The phase diagram for $t > 0$ can be studied by the mean-field approximation. The mean-field Hamiltonian is

$$H_{\text{MF}} = \sum_{i \in A} H_A + \sum_{i \in B} H_B, \quad (2)$$

$$H_A = -zt\phi_B(b_i^\dagger + b_i) + \frac{U}{2}n_i(n_i - 1) - \mu n_i + zVn_B n_i, \quad (3)$$

$$H_B = -zt\phi_A(b_i^\dagger + b_i) + \frac{U}{2}n_i(n_i - 1) - \mu n_i + zVn_A n_i. \quad (4)$$

where $\phi_A = \langle b_i \rangle_{i \in A} = \langle b_i^\dagger \rangle_{i \in A}$ and $\phi_B = \langle b_i \rangle_{i \in B} = \langle b_i^\dagger \rangle_{i \in B}$ are the expectation values of the annihilation operators on sublattices A and B , respectively. Likewise, $n_A = \langle n_i \rangle_{i \in A}$ and $n_B = \langle n_i \rangle_{i \in B}$ are the expectation values of the number operators on sublattices A and B , respectively. The expectation values are calculated numerically using the eigenstates of H_A and H_B . The phase diagram of the extended Bose-Hubbard model on a square lattice for $V/U = 0.2$ is shown in Fig. 1. For small t , the order parameters $\phi_A = \phi_B = 0$, and the ground state is the CDW state ($n_A \neq n_B$) or the MI state ($n_A = n_B$). When t exceeds the critical value t_c [23], the ground state is the SF state ($\phi_A = \phi_B > 0$) or the SS state ($\phi_A \neq \phi_B$). The SF phase exists for all $\mu \geq 0$ for large t . In contrast, the SS phase exists between the CDW and SF phase.

III. GREEN'S FUNCTION

To calculate the momentum dependence of the excitation energy and distribution function, we derive Green's functions by the standard basis operator method [12–14, 29, 31–33]. By considering fluctuations around the mean-field ground state, the Hamiltonian is written as

$$H_L = H_{\text{MF}} - t \sum_{\langle i, j \rangle} (\delta b_i^\dagger \delta b_j + \text{H.c.}), \quad (5)$$

where the operators $\delta b_i^\dagger = b_i^\dagger - \phi_i$ and $\delta b_i = b_i - \phi_i$ represent the deviations from the mean-field Hamiltonian. By using the energy eigenstates $|i, \alpha\rangle$ of the mean-field Hamiltonian at site i with eigenenergies E_α^i , Eq. (5) is rewritten as

$$H_L = \sum_{i, \alpha} E_\alpha^i \hat{L}_{\alpha\alpha}^i - t \sum_{\langle i, j \rangle} \sum_{\alpha\alpha'} \sum_{\beta\beta'} (d_{\alpha\alpha'}^i c_{\beta\beta'}^j \delta \hat{L}_{\alpha\alpha'}^i \delta \hat{L}_{\beta\beta'}^j + \text{H.c.}), \quad (6)$$

where $\hat{L}_{\alpha\alpha'}^i = |i, \alpha\rangle\langle i, \alpha'|$ is the standard basis operator (SBO) [32], $\delta \hat{L}_{\alpha\alpha'}^i = \hat{L}_{\alpha\alpha'}^i - \langle \hat{L}_{\alpha\alpha'}^i \rangle$, $d_{\alpha\alpha'}^i = \langle i, \alpha | b_i^\dagger | i, \alpha' \rangle$, and $c_{\beta\beta'}^j = \langle j, \beta | b_j | j, \beta' \rangle$. In this formalism, the retarded Green's function $G^{ij}(t-t') = -i\Theta(t-t')\langle [b_i(t), b_j^\dagger(t')] \rangle$ [34] is written as

$$G^{ij}(t-t') = \sum_{\alpha\alpha'} \sum_{\beta\beta'} c_{\alpha\alpha'}^i d_{\beta\beta'}^j G_{\alpha\alpha', \beta\beta'}^{ij}(t-t'), \quad (7)$$

where

$$G_{\alpha\alpha', \beta\beta'}^{ij}(t-t') = -i\Theta(t-t')\langle [\hat{L}_{\alpha\alpha'}^i(t), \hat{L}_{\beta\beta'}^j(t')] \rangle. \quad (8)$$

The equation for the Green's function in frequency space in random phase approximation (RPA) [12–14, 31, 33] is

$$[\omega - E_{\alpha'\alpha}^i] G_{\alpha\alpha', \beta\beta'}^{ij}(\omega) = D_{\alpha\alpha'}^i \delta_{\alpha'\beta} \delta_{\alpha\beta'} \delta^{ij} - t D_{\alpha\alpha'}^i \sum_l \sum_{\gamma\gamma'} T_{\alpha\alpha'\gamma\gamma'}^{il} G_{\gamma\gamma', \beta\beta'}^{lj}(\omega), \quad (9)$$

where $E_{\alpha'\alpha}^i = E_{\alpha'}^i - E_\alpha^i$, $T_{\alpha\alpha'\gamma\gamma'}^{il} = d_{\alpha\alpha'}^i c_{\gamma\gamma'}^l + c_{\alpha\alpha'}^i d_{\gamma\gamma'}^l$, and $D_{\alpha\alpha'}^i = D_\alpha^i - D_{\alpha'}^i$. The occupation probability $D_\alpha^i = \langle \hat{L}_{\alpha\alpha}^i \rangle$ is equal to unity when α is the ground state, and zero when α is another state at zero temperature. By solving Eq. (9), we obtain the Green's function expressed by the mean-field Green's functions

$$\begin{pmatrix} F_{cd}^i & F_{cc}^i \\ F_{dd}^i & F_{dc}^i \end{pmatrix} = \sum_{\alpha\alpha'} \frac{D_{\alpha\alpha'}^i}{\omega - E_{\alpha'\alpha}^i} \begin{pmatrix} c_{\alpha\alpha'}^i d_{\alpha'\alpha}^i & c_{\alpha\alpha'}^i c_{\alpha'\alpha}^i \\ d_{\alpha\alpha'}^i d_{\alpha'\alpha}^i & d_{\alpha\alpha'}^i c_{\alpha'\alpha}^i \end{pmatrix}. \quad (10)$$

We solve Eq. (9) for the MI, CDW, SF, and SS phases.

A. MI phase

In the MI phase ($\phi_A = \phi_B = 0$, $n_A = n_B = n$), sublattices A and B are equivalent. Thus, the Fourier transformation of the Green's function in Eq. (7) is defined as

$$G^{ij}(\omega) = \frac{1}{N} \sum_{\mathbf{k}} G_{\mathbf{k}}(\omega) e^{-i\mathbf{k} \cdot (\mathbf{R}_i - \mathbf{R}_j)}, \quad (11)$$

$$G_{\mathbf{k}}(\omega) = \frac{1}{N} \sum_{ij} G^{ij}(\omega) e^{i\mathbf{k} \cdot (\mathbf{R}_i - \mathbf{R}_j)}, \quad (12)$$

where N is the number of lattice sites. In momentum space, the equation for the Green's function is

$$G_{\mathbf{k}}(\omega) = F_{cd} + \epsilon_{\mathbf{k}} F_{cd} G_{\mathbf{k}}(\omega), \quad (13)$$

where $\epsilon_{\mathbf{k}} = -2t \sum_{i=x,y} \cos(k_i)$ and the lattice constant is set to unity. From Eq. (13), the Green's function is

$$G_{\mathbf{k}}(\omega) = F_{cd} / (1 - \epsilon_{\mathbf{k}} F_{cd}). \quad (14)$$

In the MI phase, $G_{\mathbf{k}}(\omega)$ is analytically obtained since F_{cd} is given analytically. Considering that the ground state is the number state $|i, n_i\rangle$ with $E_{n_i} = Un_i(n_i - 1)/2 - \mu n_i + zVn_i$ and $c_{n'_i n_i}^i = \sqrt{n_i} \delta_{n'_i, n_i - 1}$, the mean-field Green's function is

$$F_{cd} = \frac{n+1}{\omega - E^p} - \frac{n}{\omega + E^h}, \quad (15)$$

where $E^p = E_{n+1} - E_n = Un + zVn - \mu$ and $E^h = E_{n-1} - E_n = -U(n-1) - zVn + \mu$ are particle and hole excitation energies, respectively. By substituting Eq. (15) into Eq. (14), the Green's function is

$$G_{\mathbf{k}}(\omega) = \frac{C^p(\mathbf{k})}{\omega - E^p(\mathbf{k})} - \frac{C^h(\mathbf{k})}{\omega + E^h(\mathbf{k})}, \quad (16)$$

where $E^p(\mathbf{k}) = E^p - [U - E^U(\mathbf{k}) - \epsilon_{\mathbf{k}}]/2$, $E^h(\mathbf{k}) = E^h - [U - E^U(\mathbf{k}) + \epsilon_{\mathbf{k}}]/2$, $E^U(\mathbf{k}) = \sqrt{\epsilon_{\mathbf{k}}^2 + 2U(2n+1)\epsilon_{\mathbf{k}} + U^2}$, $C^p(\mathbf{k}) = [\epsilon_{\mathbf{k}} + (2n+1)U + E^U(\mathbf{k})]/[2E^U(\mathbf{k})]$, and $C^h(\mathbf{k}) = [\epsilon_{\mathbf{k}} + (2n+1)U - E^U(\mathbf{k})]/[2E^U(\mathbf{k})]$. The spectral function is

$$\begin{aligned} A(\mathbf{k}, \omega) &= -\frac{1}{\pi} \text{Im} G_{\mathbf{k}}(\omega + i0^+) \\ &= C^p(\mathbf{k}) \delta[\omega - E^p(\mathbf{k})] - C^h(\mathbf{k}) \delta[\omega + E^h(\mathbf{k})], \end{aligned} \quad (17)$$

where $C^p(\mathbf{k})$ is the spectral weight of the particle excitation, and $C^h(\mathbf{k})$ is that of the hole excitation. The momentum distribution is

$$n(\mathbf{k}) = - \int_{-\infty}^0 A(\mathbf{k}, \omega) d\omega = C^h(\mathbf{k}). \quad (18)$$

B. CDW phase

In the CDW phase ($\phi_A = \phi_B = 0$, $n_A \neq n_B$), sublattices A and B are inequivalent and each consists of $N/2$ lattice sites. Therefore, the Fourier transformation of Green's functions for sublattices is defined as

$$G^{i_m j_n}(\omega) = \frac{2}{N} \sum_{\mathbf{k}} G_{\mathbf{k}}^{mn}(\omega) e^{-i\mathbf{k} \cdot (\mathbf{R}_{i_m} - \mathbf{R}_{j_n})}, \quad (19)$$

$$G_{\mathbf{k}}^{mn}(\omega) = \frac{2}{N} \sum_{i_m j_n} G^{i_m j_n}(\omega) e^{i\mathbf{k} \cdot (\mathbf{R}_{i_m} - \mathbf{R}_{j_n})}, \quad (20)$$

where indices m and n label sublattices A and B [35]. The equations for the Green's functions in momentum space is

$$G_{\mathbf{k}}^{AA}(\omega) = F_{cd}^A + \epsilon_{\mathbf{k}} F_{cd}^A G_{\mathbf{k}}^{BA}(\omega), \quad (21)$$

$$G_{\mathbf{k}}^{BA}(\omega) = \epsilon_{\mathbf{k}} F_{cd}^B G_{\mathbf{k}}^{AA}(\omega), \quad (22)$$

$$G_{\mathbf{k}}^{BB}(\omega) = F_{cd}^B + \epsilon_{\mathbf{k}} F_{cd}^B G_{\mathbf{k}}^{AB}(\omega), \quad (23)$$

$$G_{\mathbf{k}}^{AB}(\omega) = \epsilon_{\mathbf{k}} F_{cd}^A G_{\mathbf{k}}^{BB}(\omega). \quad (24)$$

From these equations, the Green's functions are

$$G_{\mathbf{k}}^{AA}(\omega) = F_{cd}^A / \Delta, \quad (25)$$

$$G_{\mathbf{k}}^{BA}(\omega) = G_{\mathbf{k}}^{AB}(\omega) = \epsilon_{\mathbf{k}} F_{cd}^A F_{cd}^B / \Delta, \quad (26)$$

$$G_{\mathbf{k}}^{BB}(\omega) = F_{cd}^B / \Delta. \quad (27)$$

where $\Delta = 1 - \epsilon_{\mathbf{k}}^2 F_{cd}^A F_{cd}^B$. These Green's functions can be analytically expressed since F_{cd}^A and F_{cd}^B are given by

$$F_{cd}^A = \frac{n_A + 1}{\omega - E_A^p} - \frac{n_A}{\omega + E_A^h}, \quad (28)$$

$$F_{cd}^B = \frac{n_B + 1}{\omega - E_B^p} - \frac{n_B}{\omega + E_B^h}, \quad (29)$$

where $E_A^p = Un_A + zVn_B - \mu$, $E_A^h = -U(n_A - 1) - zVn_B + \mu$, $E_B^p = Un_B + zVn_A - \mu$, $E_B^h = -U(n_B - 1) - zVn_A + \mu$. The Green's function is

$$\begin{aligned} G_{\mathbf{k}}(\omega) &= \frac{1}{N} \sum_{ij} G^{ij}(\omega) e^{i\mathbf{k} \cdot (\mathbf{R}_i - \mathbf{R}_j)} = \frac{1}{2} \sum_{mn} G_{\mathbf{k}}^{mn}(\omega) \\ &= \frac{1}{2} [G_{\mathbf{k}}^{AA}(\omega) + G_{\mathbf{k}}^{AB}(\omega) + G_{\mathbf{k}}^{BA}(\omega) + G_{\mathbf{k}}^{BB}(\omega)]. \end{aligned} \quad (30)$$

The excitation energies are the poles of the Green's function, which are the solutions of $\Delta = 1 - \epsilon_{\mathbf{k}}^2 F_{cd}^A F_{cd}^B = 0$. It was stated in Ref. [29] that these poles were not analytically calculated since the equation is quartic in ω . However, a quartic equation can be solved by Ferrari's formula, so the poles are analytically obtained. Thus, the Green's function is written as

$$\begin{aligned} G_{\mathbf{k}}(\omega) &= \frac{C_A^p(\mathbf{k})}{\omega - E_A^p(\mathbf{k})} + \frac{C_B^p(\mathbf{k})}{\omega - E_B^p(\mathbf{k})} \\ &\quad - \frac{C_A^h(\mathbf{k})}{\omega + E_A^h(\mathbf{k})} - \frac{C_B^h(\mathbf{k})}{\omega + E_B^h(\mathbf{k})}, \end{aligned} \quad (31)$$

where the excitation energies and spectral weights can be analytically expressed, but the expressions are too long to write here. The momentum distribution is

$$n(\mathbf{k}) = - \int_{-\infty}^0 A(\mathbf{k}, \omega) d\omega = C_A^h(\mathbf{k}) + C_B^h(\mathbf{k}). \quad (32)$$

C. SF phase

In the SF phase ($\phi_A = \phi_B \neq 0$, $n_A = n_B$), it is necessary to introduce the anomalous Green's function [31] defined by

$$\begin{aligned} H^{ij}(t-t') &= -i\Theta(t-t')\langle [b_i^\dagger(t), b_j^\dagger(t')] \rangle \\ &= \sum_{\alpha\alpha'} \sum_{\beta\beta'} d_{\alpha\alpha'}^i d_{\beta\beta'}^j G_{\alpha\alpha', \beta\beta'}^{ij}(t-t'). \end{aligned} \quad (33)$$

The equations for the Green's functions are

$$G_{\mathbf{k}}(\omega) = F_{cd} + \epsilon_{\mathbf{k}} F_{cc} H_{\mathbf{k}}(\omega) + \epsilon_{\mathbf{k}} F_{cd} G_{\mathbf{k}}(\omega), \quad (34)$$

$$H_{\mathbf{k}}(\omega) = F_{dd} + \epsilon_{\mathbf{k}} F_{dc} H_{\mathbf{k}}(\omega) + \epsilon_{\mathbf{k}} F_{dd} G_{\mathbf{k}}(\omega). \quad (35)$$

From these equations,

$$G_{\mathbf{k}}(\omega) = (F_{cd} - \epsilon_{\mathbf{k}} F_{cd} F_{dc} + \epsilon_{\mathbf{k}} F_{cc} F_{dd}) / \Delta, \quad (36)$$

$$H_{\mathbf{k}}(\omega) = F_{dd} / \Delta, \quad (37)$$

where

$$\Delta = 1 - \epsilon_{\mathbf{k}} F_{cd} - \epsilon_{\mathbf{k}} F_{dc} + \epsilon_{\mathbf{k}}^2 F_{cd} F_{dc} - \epsilon_{\mathbf{k}}^2 F_{cc} F_{dd}. \quad (38)$$

When $V = 0$, the Equation (36) is the same as $G_{\mathbf{k}}(\omega) = \Pi_{\mathbf{k}}(\omega) / [1 - \epsilon_{\mathbf{k}} \Pi_{\mathbf{k}}(\omega)]$, where $\Pi_{\mathbf{k}}(\omega) = F_{cd} + \epsilon_{\mathbf{k}} F_{cc} F_{dd} / (1 - \epsilon_{\mathbf{k}} F_{dc})$ [13, 14, 31]. In contrast to the insulating phases, the mean-field Green's functions can not be obtained analytically, so the Green's function is also obtained numerically. To obtain the excitation energies and spectral weights, we factor the numerator and denominator of the Green's function and then cancel out common terms numerically. Consequently, the Green's function is decomposed as

$$G_{\mathbf{k}}(\omega) = \sum_{\alpha} \frac{C_{\alpha}^p(\mathbf{k})}{\omega - E_{\alpha}^p(\mathbf{k})} - \sum_{\alpha} \frac{C_{\alpha}^h(\mathbf{k})}{\omega + E_{\alpha}^h(\mathbf{k})}. \quad (39)$$

The number of the poles of the Green's function is the same as that of the mean-field Green's functions. When the mean-field Hamiltonian is diagonalized in the occupation number basis $\{|0\rangle, |1\rangle, \dots, |n_{\max}\rangle\}$, the number of the poles are $2n_{\max}$ at zero temperature. The momentum distribution is $n(\mathbf{k}) = \sum_{\alpha} C_{\alpha}^h(\mathbf{k})$.

D. SS phase

We derive Green's functions in the SS phase ($\phi_A \neq \phi_B$, $n_A \neq n_B$). The equations for the Green's functions are

$$G_{\mathbf{k}}^{BB}(\omega) = F_{cd}^B + \epsilon_{\mathbf{k}} F_{cd}^B G_{\mathbf{k}}^{AB}(\omega) + \epsilon_{\mathbf{k}} F_{cc}^B H_{\mathbf{k}}^{AB}(\omega), \quad (40)$$

$$G_{\mathbf{k}}^{AB}(\omega) = \epsilon_{\mathbf{k}} F_{cd}^A G_{\mathbf{k}}^{BB}(\omega) + \epsilon_{\mathbf{k}} F_{cc}^A H_{\mathbf{k}}^{BB}(\omega), \quad (41)$$

$$H_{\mathbf{k}}^{BB}(\omega) = F_{dd}^B + \epsilon_{\mathbf{k}} F_{dc}^B H_{\mathbf{k}}^{AB}(\omega) + \epsilon_{\mathbf{k}} F_{dd}^B G_{\mathbf{k}}^{AB}(\omega), \quad (42)$$

$$H_{\mathbf{k}}^{AB}(\omega) = \epsilon_{\mathbf{k}} F_{dc}^A H_{\mathbf{k}}^{BB}(\omega) + \epsilon_{\mathbf{k}} F_{dd}^A G_{\mathbf{k}}^{BB}(\omega), \quad (43)$$

$$G_{\mathbf{k}}^{AA}(\omega) = F_{cd}^A + \epsilon_{\mathbf{k}} F_{cd}^A G_{\mathbf{k}}^{BA}(\omega) + \epsilon_{\mathbf{k}} F_{cc}^A H_{\mathbf{k}}^{BA}(\omega), \quad (44)$$

$$G_{\mathbf{k}}^{BA}(\omega) = \epsilon_{\mathbf{k}} F_{cd}^B G_{\mathbf{k}}^{AA}(\omega) + \epsilon_{\mathbf{k}} F_{cc}^B H_{\mathbf{k}}^{AA}(\omega), \quad (45)$$

$$H_{\mathbf{k}}^{AA}(\omega) = F_{dd}^A + \epsilon_{\mathbf{k}} F_{dc}^A H_{\mathbf{k}}^{BA}(\omega) + \epsilon_{\mathbf{k}} F_{dd}^A G_{\mathbf{k}}^{BA}(\omega), \quad (46)$$

$$H_{\mathbf{k}}^{BA}(\omega) = \epsilon_{\mathbf{k}} F_{dc}^B H_{\mathbf{k}}^{AA}(\omega) + \epsilon_{\mathbf{k}} F_{dd}^B G_{\mathbf{k}}^{AA}(\omega). \quad (47)$$

From Eqs. (40)–(43), the Green's functions are

$$G_{\mathbf{k}}^{BB}(\omega) = (F_{cd}^B - \epsilon_{\mathbf{k}}^2 F_{dc}^A F_{cd}^B F_{dc}^B + \epsilon_{\mathbf{k}}^2 F_{dc}^A F_{cc}^B F_{dd}^B) / \Delta, \quad (48)$$

$$\begin{aligned} G_{\mathbf{k}}^{AB}(\omega) &= \epsilon_{\mathbf{k}} (F_{cd}^A F_{cd}^B + F_{cc}^A F_{dd}^B - \epsilon_{\mathbf{k}}^2 F_{cd}^A F_{dc}^A F_{cd}^B F_{dc}^B \\ &\quad - \epsilon_{\mathbf{k}}^2 F_{cc}^A F_{dd}^B F_{cc}^B F_{dd}^B + \epsilon_{\mathbf{k}}^2 F_{cc}^A F_{dd}^A F_{cd}^B F_{dc}^B \\ &\quad + \epsilon_{\mathbf{k}}^2 F_{cd}^A F_{dc}^A F_{cc}^B F_{dd}^B) / \Delta, \end{aligned} \quad (49)$$

$$H_{\mathbf{k}}^{BB}(\omega) = (F_{dd}^B + \epsilon_{\mathbf{k}}^2 F_{dd}^A F_{cd}^B F_{dc}^B - \epsilon_{\mathbf{k}}^2 F_{dd}^A F_{cc}^B F_{dd}^B) / \Delta, \quad (50)$$

$$H_{\mathbf{k}}^{AB}(\omega) = \epsilon_{\mathbf{k}} (F_{dd}^A F_{cd}^B + F_{dc}^A F_{dd}^B) / \Delta, \quad (51)$$

where

$$\begin{aligned} \Delta &= 1 - \epsilon_{\mathbf{k}}^2 F_{cd}^A F_{cd}^B - \epsilon_{\mathbf{k}}^2 F_{dc}^A F_{dc}^B - \epsilon_{\mathbf{k}}^2 F_{dd}^A F_{cc}^B - \epsilon_{\mathbf{k}}^2 F_{cc}^A F_{dd}^B \\ &\quad + \epsilon_{\mathbf{k}}^4 F_{cd}^A F_{dc}^A F_{cd}^B F_{dc}^B + \epsilon_{\mathbf{k}}^4 F_{cc}^A F_{dd}^A F_{cc}^B F_{dd}^B \\ &\quad - \epsilon_{\mathbf{k}}^4 F_{cc}^A F_{dd}^A F_{cd}^B F_{dc}^B - \epsilon_{\mathbf{k}}^4 F_{cd}^A F_{dc}^A F_{cc}^B F_{dd}^B. \end{aligned} \quad (52)$$

$G_{\mathbf{k}}^{AA}(\omega)$, $G_{\mathbf{k}}^{BA}(\omega)$, $H_{\mathbf{k}}^{AA}(\omega)$, and $H_{\mathbf{k}}^{BA}(\omega)$ are derived from $G_{\mathbf{k}}^{BB}(\omega)$, $G_{\mathbf{k}}^{AB}(\omega)$, $H_{\mathbf{k}}^{BB}(\omega)$, and $H_{\mathbf{k}}^{AB}(\omega)$ by interchanging the subscripts A and B , respectively. The Green's function is $G_{\mathbf{k}}(\omega) = [G_{\mathbf{k}}^{AA}(\omega) + G_{\mathbf{k}}^{AB}(\omega) + G_{\mathbf{k}}^{BA}(\omega) + G_{\mathbf{k}}^{BB}(\omega)] / 2$. Like the SF phase, the Green's function is decomposed as

$$\begin{aligned} G_{\mathbf{k}}(\omega) &= \sum_{\alpha} \frac{C_{A,\alpha}^p(\mathbf{k})}{\omega - E_{A,\alpha}^p(\mathbf{k})} + \sum_{\alpha} \frac{C_{B,\alpha}^p(\mathbf{k})}{\omega - E_{B,\alpha}^p(\mathbf{k})} \\ &\quad - \sum_{\alpha} \frac{C_{A,\alpha}^h(\mathbf{k})}{\omega + E_{A,\alpha}^h(\mathbf{k})} - \sum_{\alpha} \frac{C_{B,\alpha}^h(\mathbf{k})}{\omega + E_{B,\alpha}^h(\mathbf{k})}. \end{aligned} \quad (53)$$

The momentum distribution is $n(\mathbf{k}) = \sum_{\alpha} C_{A,\alpha}^h(\mathbf{k}) + \sum_{\alpha} C_{B,\alpha}^h(\mathbf{k})$.

IV. EXCITATION SPECTRUM

The excitation spectrum is given by the poles of the Green's function. Figure 2 shows the excitation spectrum of the extended Bose-Hubbard model on a square lattice for $U = 1$ and $V/U = 0.2$ for the MI, CDW, SF, and SS

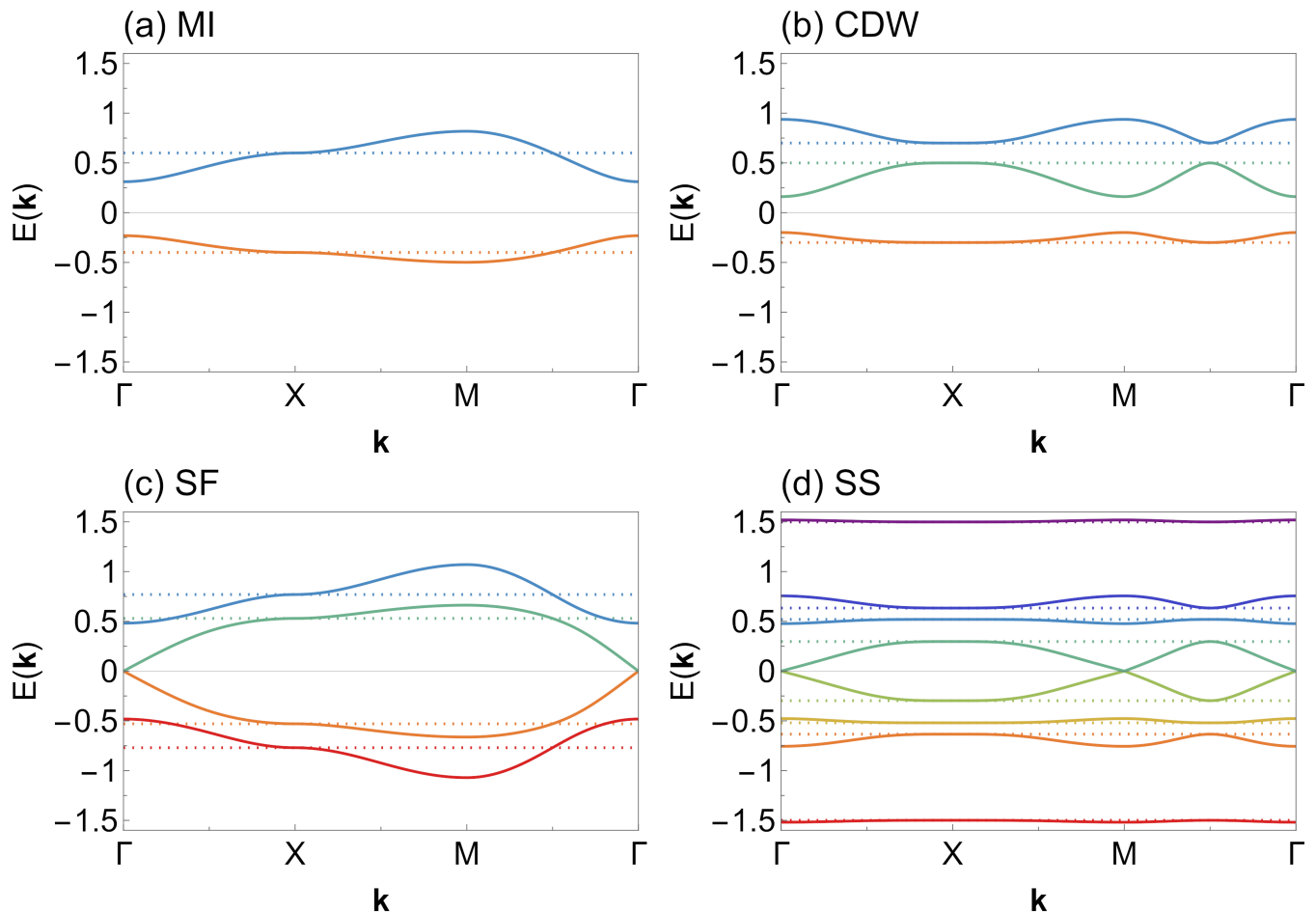


FIG. 2. Excitation spectrum of the extended Bose-Hubbard model on a square lattice for $U = 1$ and $V/U = 0.2$ at zero temperature for (a) MI ($t/U = 0.03$, $\mu/U = 1.2$), (b) CDW ($t/U = 0.06$, $\mu/U = 0.3$), (c) SF ($t/U = 0.06$, $\mu/U = 1.2$), and (d) SS ($t/U = 0.06$, $\mu/U = 0.6$). The points Γ , X, and M are $(0,0)$, $(\pi,0)$, and (π,π) , respectively. The solid lines are excitation energies calculated by the standard basis operator method, and the dotted lines are mean-field excitation energies.

phases. Positive and negative excitation energies are particle and hole excitation energies, respectively. In all the phases, the excitation energy calculated by the standard basis operator method agrees with the mean-field excitation energy at X, where the correction to the mean-field result is zero since $\epsilon_{\mathbf{k}} = 0$ at X. In the MI phase, the spectrum is gapped for all \mathbf{k} . The particle excitation energy increases along Γ -X-M since $E^p(\mathbf{k})$ is a monotonically increasing function of $\epsilon_{\mathbf{k}}$. The MI-SF phase transition occurs when either $E^p(\mathbf{k} = \Gamma)$ or $E^h(\mathbf{k} = \Gamma)$ becomes zero, which determines the MI-SF phase boundary. In the CDW phase, the hole excitation on sublattice B is not possible since $n_B = 0$. Thus, the particle excitations on sublattices A and B and the hole excitation on sublattice A are shown. The excitation energy is a function of $\epsilon_{\mathbf{k}}^2$, so the excitation spectrum along Γ -X is the same as that along M-X. This characteristic structure was not observed in Ref. [28]. In the SF phase, there are Goldstone modes, which are gapless and linear around Γ . In addition to gapless modes, there exist gapped modes, which

can not be calculated by theories of weakly interacting bosons. Like the MI phase, the particle excitation energies increase along Γ -X-M. In the SS phase, since the excitation energy is a function of $\epsilon_{\mathbf{k}}^2$ and $\epsilon_{\mathbf{k}}^4$, the spectrum is gapless and linear around M as well as Γ . The gapless excitation at M reflects the simultaneous presence of superfluidity and solidity.

V. MOMENTUM DISTRIBUTION

The momentum distribution is given by the sum of the spectral weights of the hole excitations. Figure 3 shows the momentum distribution of the extended Bose-Hubbard model on a square lattice for $U = 1$ and $V/U = 0.2$ for the MI, CDW, SF, and SS phases. In the MI phase, the momentum distribution decreases along Γ -X-M because $n(\mathbf{k})$ is a monotonically decreasing function of $\epsilon_{\mathbf{k}}$. In the CDW phase, in addition to a large peak at Γ , there is a small peak at M. This peak does not exist in

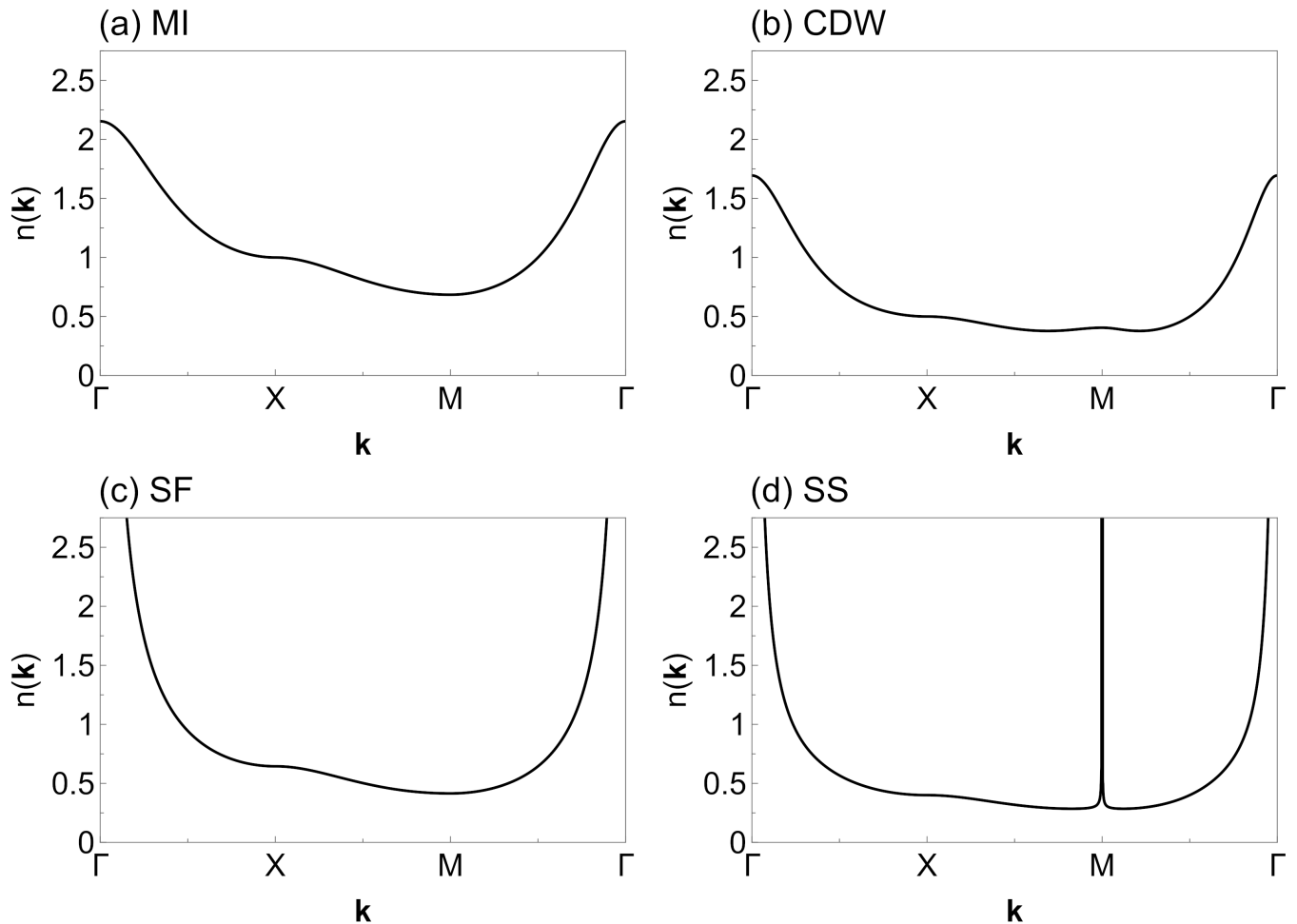


FIG. 3. Momentum distribution of the extended Bose-Hubbard model on a square lattice for $U = 1$ and $V/U = 0.2$ at zero temperature for (a) MI ($t/U = 0.03$, $\mu/U = 1.2$), (b) CDW ($t/U = 0.06$, $\mu/U = 0.3$), (c) SF ($t/U = 0.06$, $\mu/U = 1.2$), and (d) SS ($t/U = 0.06$, $\mu/U = 0.6$).

the MI phase. However, it is pointed out that a peak at M appears only close to the CDW-SS phase boundary [29]. The critical value t_m where $n(\mathbf{k})$ at M becomes a local maximum is the value which satisfies $dn(\mathbf{k} = M)/dt = 0$. In the SF phase, the momentum distribution increases drastically as \mathbf{k} approaches Γ and diverges at Γ . This divergent peak at zero momentum indicates the existence of Bose-Einstein condensation. In the SS phase, the momentum distribution increases more sharply around M than around Γ and diverges at M. A peak at M is also observed in quantum Monte Carlo simulations [30]. This peak indicates the coexistence of superfluid and solid order.

VI. CONCLUSIONS

By the standard operator method, we have derived Green's functions of the extended Bose-Hubbard model in MI, CDW, SF, and SS phases. The excitation spectrum has gapped modes in all the phases and gapless Goldstone modes in the SF and SS phases. The momentum distribution has a peak at Γ in all the phases and a peak at M in the SS phase and the CDW phase close to the CDW-SS phase boundary. These quantities have been calculated at zero temperature, so calculations at finite temperatures should be the subject of further study. The SBO method developed in this study will be applied to other lattices.

ACKNOWLEDGMENTS

This work was supported by JST SPRING, Grant Number JPMJSP2108.

-
- [1] M. P. Fisher, P. B. Weichman, G. Grinstein, and D. S. Fisher, Boson localization and the superfluid-insulator transition, *Physical Review B* **40**, 546 (1989).
- [2] D. Jaksch, C. Bruder, J. I. Cirac, C. W. Gardiner, and P. Zoller, Cold bosonic atoms in optical lattices, *Physical Review Letters* **81**, 3108 (1998).
- [3] J. Freericks and H. Monien, Phase diagram of the bose-hubbard model, *EPL (Europhysics Letters)* **26**, 545 (1994).
- [4] D. Van Oosten, P. van der Straten, and H. Stoof, Quantum phases in an optical lattice, *Physical Review A* **63**, 053601 (2001).
- [5] B. Capogrosso-Sansone, N. Prokof'Ev, and B. Svistunov, Phase diagram and thermodynamics of the three-dimensional bose-hubbard model, *Physical Review B* **75**, 134302 (2007).
- [6] K. Sengupta and N. Dupuis, Mott-insulator-to-superfluid transition in the bose-hubbard model: A strong-coupling approach, *Physical Review A* **71**, 033629 (2005).
- [7] S. D. Huber, E. Altman, H. P. Büchler, and G. Blatter, Dynamical properties of ultracold bosons in an optical lattice, *Physical Review B* **75**, 085106 (2007).
- [8] K. V. Krutitsky and P. Navez, Excitation dynamics in a lattice bose gas within the time-dependent gutzwiller mean-field approach, *Physical Review A* **84**, 033602 (2011).
- [9] M. Di Liberto, A. Recati, N. Trivedi, I. Carusotto, and C. Menotti, Particle-hole character of the higgs and goldstone modes in strongly interacting lattice bosons, *Physical review letters* **120**, 073201 (2018).
- [10] F. Caleffi, M. Capone, C. Menotti, I. Carusotto, and A. Recati, Quantum fluctuations beyond the gutzwiller approximation in the bose-hubbard model, *Physical Review Research* **2**, 033276 (2020).
- [11] A. Dutta, C. Trefzger, and K. Sengupta, Projection operator approach to the bose-hubbard model, *Physical Review B* **86**, 085140 (2012).
- [12] K. Sheshadri, H. Krishnamurthy, R. Pandit, and T. Ramakrishnan, Superfluid and insulating phases in an interacting-boson model: Mean-field theory and the rpa, *EPL (Europhysics Letters)* **22**, 257 (1993).
- [13] Y. Ohashi, M. Kitaura, and H. Matsumoto, Itinerant-localized dual character of a strongly correlated superfluid bose gas in an optical lattice, *Physical Review A* **73**, 033617 (2006).
- [14] C. Menotti and N. Trivedi, Spectral weight redistribution in strongly correlated bosons in optical lattices, *Physical Review B* **77**, 235120 (2008).
- [15] Y. Kato, Q. Zhou, N. Kawashima, and N. Trivedi, Sharp peaks in the momentum distribution of bosons in optical lattices in the normal state, *Nature Physics* **4**, 617 (2008).
- [16] J. Freericks, H. Krishnamurthy, Y. Kato, N. Kawashima, and N. Trivedi, Strong-coupling expansion for the momentum distribution of the bose-hubbard model with benchmarking against exact numerical results, *Physical Review A* **79**, 053631 (2009).
- [17] M. Knap, E. Arrigoni, and W. von der Linden, Spectral properties of strongly correlated bosons in two-dimensional optical lattices, *Physical Review B* **81**, 024301 (2010).
- [18] O. Dutta, M. Gajda, P. Hauke, M. Lewenstein, D.-S. Lühmann, B. A. Malomed, T. Sowiński, and J. Zakrzewski, Non-standard hubbard models in optical lattices: a review, *Reports on Progress in Physics* **78**, 066001 (2015).
- [19] G. Batrouni, R. Scalettar, G. Zimanyi, and A. P. Kampf, Supersolids in the bose-hubbard hamiltonian, *Physical review letters* **74**, 2527 (1995).
- [20] P. Sengupta, L. P. Pryadko, F. Alet, M. Troyer, and G. Schmid, Supersolids versus phase separation in two-dimensional lattice bosons, *Physical review letters* **94**, 207202 (2005).
- [21] D. L. Kovrizhin, G. V. Pai, and S. Sinha, Density wave and supersolid phases of correlated bosons in an optical lattice, *EPL (Europhysics Letters)* **72**, 162 (2005).
- [22] K. Yamamoto, S. Todo, and S. Miyashita, Successive phase transitions at finite temperatures toward the supersolid state in a three-dimensional extended bose-hubbard model, *Physical Review B* **79**, 094503 (2009).
- [23] M. Iskin, Route to supersolidity for the extended bose-hubbard model, *Physical Review A* **83**, 051606 (2011).
- [24] T. Kimura, Gutzwiller study of extended hubbard models with fixed boson densities, *Physical Review A* **84**, 063630 (2011).
- [25] D. Rossini and R. Fazio, Phase diagram of the extended bose-hubbard model, *New Journal of Physics* **14**, 065012 (2012).
- [26] T. Ohgoe, T. Suzuki, and N. Kawashima, Commensurate supersolid of three-dimensional lattice bosons, *Physical Review Letters* **108**, 185302 (2012).
- [27] B. Grémaud and G. G. Batrouni, Excitation and dynamics in the extended bose-hubbard model, *Physical Review B* **93**, 035108 (2016).
- [28] J. M. Kurdestany, R. V. Pai, and R. Pandit, Random-phase-approximation excitation spectra for bose-hubbard models, *arXiv preprint arXiv:1410.3621* (2014).
- [29] M. Iskin and J. Freericks, Momentum distribution of the insulating phases of the extended bose-hubbard model, *Physical Review A* **80**, 063610 (2009).
- [30] T. Ohgoe, T. Suzuki, and N. Kawashima, Ground-state phase diagram of the two-dimensional extended bose-hubbard model, *Physical Review B* **86**, 054520 (2012).
- [31] A. Sajna, T. Polak, R. Micnas, and P. Rożek, Ground-state and finite-temperature properties of correlated ultracold bosons on optical lattices, *Physical Review A* **92**, 013602 (2015).
- [32] S. B. Haley and P. Erdős, Standard-basis operator method in the green's-function technique of many-body systems with an application to ferromagnetism, *Physical Review B* **5**, 1106 (1972).
- [33] S. Konabe, T. Nikuni, and M. Nakamura, Laser probing of the single-particle energy gap of a bose gas in an optical lattice in the mott-insulator phase, *Physical Review A* **73**, 033621 (2006).
- [34] D. N. Zubarev, Double-time green functions in statistical physics, *Soviet Physics Uspekhi* **3**, 320 (1960).
- [35] P. Fröbrich and P.-J. Kuntz, Many-body green's function theory of heisenberg films, *Physics Reports* **432**, 223 (2006).